Journal of Visualized Experiments

Standardized Data Acquisition for Neuromelanin-sensitive Magnetic Resonance Imaging of the Substantia Nigra

--Manuscript Draft--

Article Type:	Invited Methods Article - JoVE Produced Video
Manuscript Number:	JoVE62493R2
Full Title:	Standardized Data Acquisition for Neuromelanin-sensitive Magnetic Resonance Imaging of the Substantia Nigra
Corresponding Author:	Kenneth Wengler Columbia University New York, NY UNITED STATES
Corresponding Author's Institution:	Columbia University
Corresponding Author E-Mail:	Kenneth.Wengler@nyspi.columbia.edu
Order of Authors:	Garrett Salzman
	Jocelyn Kim
	Guillermo Horga
	Kenneth Wengler
Additional Information:	
Question	**Response**
Please indicate whether this article will be Standard Access or Open Access.	Standard Access (US$2,400)
Please specify the section of the submitted manuscript.	Neuroscience
Please indicate the **city, state/province, and country** where this article will be **filmed**. Please do not use abbreviations.	New York, NY, USA
Please confirm that you have read and agree to the terms and conditions of the author license agreement that applies below:	I agree to the Author License Agreement
Please provide any comments to the journal here.	
Please indicate whether this article will be Standard Access or Open Access.	Open Access ($3900)
Please confirm that you have read and agree to the terms and conditions of the video release that applies below:	I agree to the Video Release

Powered by Editorial Manager® and ProduXion Manager® from Aries Systems Corporation

Manuscript Click here to access/download;Manuscript;62493_R2.docx

TITLE:

Standardized Data Acquisition for Neuromelanin-sensitive Magnetic Resonance Imaging of the Substantia Nigra

AUTHORS AND AFFILIATIONS:

Garrett Salzman[1], Jocelyn Kim[1], Guillermo Horga[1,2,*], Kenneth Wengler[1,2,*]

[1]New York State Psychiatric Institute, New York, NY, USA
[2]Department of Psychiatry, Columbia University, New York, NY, USA

*These authors contributed equally.

Email addresses of co-authors:

Garrett Salzman (garrett.salzman97@gmail.com)
Jocelyn Kim (Jocelyn.Kim@nyspi.columbia.edu)

Corresponding authors

Kenneth Wengler (Kenneth.Wengler@nyspi.columbia.edu)
Guillermo Horga (HorgaG@nyspi.columbia.edu)

SUMMARY:

This protocol shows how to acquire neuromelanin-sensitive magnetic resonance imaging data of the substantia nigra.

ABSTRACT:

The dopaminergic system plays a crucial role in healthy cognition (e.g., reward learning and uncertainty) and neuropsychiatric disorders (e.g., Parkinson's disease and schizophrenia). Neuromelanin is a byproduct of dopamine synthesis that accumulates in dopaminergic neurons of the substantia nigra. Neuromelanin-sensitive magnetic resonance imaging (NM-MRI) is a noninvasive method for measuring neuromelanin in those dopaminergic neurons, providing a direct measure of dopaminergic cell loss in the substantia nigra and a proxy measure of dopamine function. Although NM-MRI has been shown to be useful for studying various neuropsychiatric disorders, it is challenged by a limited field-of-view in the inferior–superior direction resulting in the potential loss of data from the accidental exclusion of part of the substantia nigra. In addition, the field is lacking a standardized protocol for the acquisition of NM-MRI data, a critical step in facilitating large-scale multisite studies and translation into the clinic. This protocol describes a step-by-step NM-MRI volume placement procedure and online quality control checks to ensure the acquisition of good-quality data covering the entire substantia nigra.

INTRODUCTION:

Neuromelanin (NM) is a dark pigment found in dopaminergic neurons of the substantia nigra (SN) and noradrenergic neurons of the locus coeruleus (LC)[1,2]. NM is synthesized by the iron-dependent oxidation of cytosolic dopamine and norepinephrine and is stored in autophagic

vacuoles in the soma[3]. It first appears in humans around 2–3 years of age and accumulates with age[1,4,5].

Within the NM-containing vacuoles of SN and LC neurons, NM forms complexes with iron. These NM-iron complexes are paramagnetic, allowing for noninvasive visualization of NM using magnetic resonance imaging (MRI)[6,7]. MRI scans that can visualize NM are known as NM-sensitive MRI (NM-MRI) and use either direct or indirect magnetization transfer effects to provide contrast between regions with high NM concentration (e.g., the SN) and the surrounding white matter[8,9].

Magnetization transfer contrast is the result of the interaction between macromolecular-bound water protons (which are saturated by the magnetization transfer pulses) and the surrounding free water protons. In NM-MRI, it is believed that the paramagnetic nature of NM-iron complexes shortens the T_1 of the surrounding free water protons, resulting in reduced magnetization-transfer effects so that regions with higher NM concentration appear hyperintense on NM-MRI scans[10]. Conversely, the white matter surrounding the SN has a high macromolecular content, resulting in large magnetization-transfer effects so that these regions appear hypointense on NM-MRI scans, thus providing high contrast between the SN and surrounding white matter.

In the SN, NM-MRI can provide a marker of dopaminergic cell loss[11] and dopamine system function[12]. These two processes are relevant for several neuropsychiatric disorders and are supported by a vast body of clinical and preclinical work. For example, abnormalities in dopamine function have been widely observed in schizophrenia; *in vivo* studies using positron emission tomography (PET) have shown increased striatal dopamine release[13-16] and increased dopamine synthesis capacity[17-22]. Furthermore, post-mortem studies have shown that patients with schizophrenia have increased levels of tyrosine hydroxylase—the rate-limiting enzyme involved in dopamine synthesis—in the basal ganglia[23] and SN[24,25].

Several studies have investigated patterns of dopaminergic cell loss, particularly in Parkinson's disease. Post-mortem studies have revealed that the pigmented dopaminergic neurons of the SN are the primary site of neurodegeneration in Parkinson's disease[26,27], and that, while SN cell loss in Parkinson's disease is not correlated with cell loss in normal aging[28], it is correlated with the duration of the disease[29]. Unlike most methods for investigating the dopaminergic system, the non-invasiveness, cost-effectiveness, and lack of ionizing radiation make NM-MRI a versatile biomarker[30].

The NM-MRI protocol described in this paper was developed to increase both within-subject and across-subject reproducibility of NM-MRI. This protocol ensures full coverage of the SN despite the limited coverage of NM-MRI scans in the inferior–superior direction. The protocol makes use of sagittal, coronal, and axial three-dimensional (3D) T1-weighted (T1w) images, and the steps should be followed to achieve proper slice stack placement. The protocol outlined in this paper has been utilized in multiple studies[31,32] and was extensively tested. Wengler et al. completed a study of the reliability of this protocol in which NM-MRI images were acquired twice in each participant across multiple days[32]. Intra-class correlation coefficients demonstrated excellent

test-retest reliability of this method for region of interest (ROI)-based and voxelwise analyses, as well as high contrast in the images.

PROTOCOL:

NOTE: The research conducted to develop this protocol was performed in compliance with New York State Psychiatric Institute Institutional Review Board guidelines (IRB #7655). One subject was scanned for recording the protocol video, and written informed consent was obtained. Refer to the **Table of Materials** for details about the MRI scanner used in this protocol.

1. MRI acquisition parameters

1.1. Acquire high-resolution T1w images using a 3D magnetization prepared rapid acquisition gradient echo (MPRAGE) sequence with the following parameters: spatial resolution = 0.8 x 0.8 x 0.8 mm^3; field-of-view (FOV) = 176 x 240 x 240 mm^3; echo time (TE) = 3.43 ms; repetition time (TR) = 2462 ms; inversion time (TI) = 1060 ms; flip angle = 8°; in-plane parallel imaging factor (ARC) = 2; through-plane parallel imaging factor (ARC) = 2^{33}; bandwidth = 208 Hz/pixel; total acquisition time = 6 min 39 s.

1.2. Acquire NM-MRI images using a two-dimensional (2D) gradient recalled echo sequence with magnetization transfer contrast (2D GRE-MTC) with the following parameters: resolution = 0.43 x 0.43 mm^2; FOV = 220 x 220 mm^2; slice-thickness = 1.5 mm; 20 slices; slice gap = 0 mm; TE = 4.8 ms; TR = 500 ms; flip angle = 40°; bandwidth = 122 Hz/pixel; MT frequency offset = 1.2 kHz; MT pulse duration = 8 ms; MT flip angle = 670°; number of averages = 5; total acquisition time = 10 min 4 s.

NOTE: Although the displayed results used these MRI acquisition parameters, this protocol is valid for various T1w and NM-MRI imaging protocols. The NM-MRI protocol should cover ~25 mm in the inferior–superior direction to guarantee complete coverage of the SN.

2. Placement of NM-MRI volume

2.1. Acquire a high-resolution T1w image (≤1 mm isotropic voxel size) that is aligned along the anterior commissure-posterior commissure (AC-PC) line and the midline. Perform the alignment of the high-resolution T1w image through online reformatting directly after image acquisition.

2.1.1. Carry out online reformatting using the vendor-provided software (e.g., if acquiring data on a GE scanner: MultiPlanar Reconstruction (MPR) in **Planning**; if acquiring data on a Siemens scanner: MPR in the **3D Task Card**; if acquiring data on a Philips scanner: MPR in the **Render Mode** of the **VolumeView Package**).

2.1.1.1. Create multiplanar reconstructions of the 3D T1w image in the axial plane perpendicular to the AC-PC line to cover the whole brain with minimal slice-gap.

2.1.1.2. Create multiplanar reconstructions of the 3D T1w image in the coronal plane perpendicular to the AC-PC line to cover the whole brain with minimal slice-gap.

2.1.1.3. Create multiplanar reconstructions of the 3D T1w image in the sagittal plane parallel to the AC-PC line to cover the whole brain with minimal slice-gap.

2.2. Load the sagittal, coronal, and axial views of the AC-PC aligned high-resolution T1w image and ensure that reference lines depicting the location of each displayed slice are present.

2.3. Identify the sagittal image that shows the largest separation between the midbrain and thalamus (**Figure 1A**). To do this, visually inspect the sagittal slices of the reformatted T1w image until the slice showing this greatest separation is identified.

2.4. Using the sagittal image from the end of step 2.3, visually identify the coronal plane that delineates the most anterior aspect of the midbrain (**Figure 1B**).

2.5. Using the coronal image from the end of step 2.4, visually identify the axial plane that delineates the inferior aspect of the third ventricle (**Figure 1C**).

2.6. On the sagittal image from the end of step 2.3, align the superior boundary of the NM-MRI volume to the axial plane identified in step 2.5 (**Figure 1D**).

2.7. Move the superior boundary of the NM-MRI volume 3 mm in the superior direction (**Figure 1E**).

2.8. Align the NM-MRI volume to the midline in the axial and coronal images (**Figure 1F**).

[Place **Figure 1** here]

3. Quality control checks

3.1. Ensure that the acquired NM-MRI images cover the entire SN and that the SN is visible in the central images but not in the most superior or most inferior images of the NM-MRI volume. Otherwise (**Figure 2**), repeat steps 2.3–2.8 to ensure correct NM-MRI volume placement. If the participant has moved significantly since the acquisition of the high-resolution T1w scan, repeat steps 2.1–2.8.

[Place **Figure 2** here]

3.2. Check for artifacts, particularly ones that go through the SN and the surrounding white matter, by visually inspecting each slice of the acquired NM-MRI scan.

3.2.1. Look for abrupt changes in signal intensity with a linear pattern that does not respect normal anatomical boundaries. For example, this may appear as a low-intensity region that is flanked by two high-intensity regions.

3.2.2. If the artifact is the result of blood vessels (**Figure 3A**), retain the NM-MRI images because these artifacts will most likely always be present.

3.2.3. If the artifacts are the result of participant head motion (**Figure 3B**), remind the participant to stay as still as possible and reacquire the NM-MRI images.

3.2.4. If the artifacts are ambiguous (**Figure 3C**), reacquire the NM-MRI images. Upon reacquisition, if the artifacts remain present, proceed with these images as they are likely biological rather than a result of motion.

3.2.5. If the NM-MRI images pass the quality control check in step 3.1, copy the previous NM-MRI volume placement. If the NM-MRI images fail the quality control check in step 3.1, repeat steps 2.3–2.8 to ensure correct NM-MRI volume placement (or steps 2.1–2.8 if the participant moved significantly).

[Place **Figure 3** here]

REPRESENTATIVE RESULTS:

Figure 4 shows the representative results from a 28-year-old female participant with no psychiatric or neurological disorders. The NM-MRI protocol ensures complete coverage of the SN, achieved by following the steps outlined in **Figure 1**, and satisfactory NM-MRI images. Excellent contrast between the SN and neighboring white matter regions with negligible NM concentration (i.e., crus cerebri) can be seen. These images were checked immediately after acquisition to ensure the proper coverage of the SN and to check for artifacts. Because full coverage of the SN was achieved without any artifacts, the scan passed the quality checks and did not need to be repeated.

[Place **Figure 4** here]

Figure 2 shows the representative results from a 28-year-old female participant with no psychiatric or neurological disorders whose images failed the first quality control check (step 3.1). The SN is visible in the most superior slice (slice 20), indicating that full coverage of the SN was not achieved. In this instance, the data must be reacquired by repeating steps 2.3–2.8 of the protocol, as shown in **Figure 1**. If the participant has moved significantly since the acquisition of the initial T1w image, then the researcher should return to step 1.1 to reacquire the T1w image.

Figure 3 shows example images that failed the second quality control check (step 3.2). As outlined in step 3.2, scans containing artifacts due to blood vessels (**Figure 3A**) do not need to be repeated, as those artifacts will likely be present in every acquisition. Scans that contain artifacts resulting from motion (**Figure 3B**) or ambiguous artifacts (**Figure 3C**) should be repeated. If the artifacts

remain present after reacquisition, then the scan does not need to be reacquired further as the artifacts are likely biological and therefore, will be present in every acquisition.

FIGURE LEGENDS:

Figure 1: Images displaying the step-by-step NM-MRI volume placement procedure. Yellow lines indicate the location of the slices used for volume placement as described in the protocol. (**A**) First, the sagittal image with the greatest separation between the midbrain and thalamus is identified (step 2.3 of the protocol). (**B**) Second, using the image from **A**, the coronal plane delineating the most anterior aspect of the midbrain is identified (step 2.4). (**C**) Third, on the coronal image from the plane identified in **B,** the axial plane delineating the inferior aspect of the third ventricle is identified (step 2.5). (**D**) Fourth, the axial plane identified in **C** is displayed on the sagittal image from **A** (step 2.6). (**E**) Fifth, the axial plane from **D** is shifted 3 mm in the superior direction, and this plane indicates the superior boundary of the NM-MRI volume (step 2.7). (**F**) The final NM-MRI volume placement where the coronal image corresponds to **C**, the sagittal image corresponds to **A**, and the axial image corresponds to the axial plane in **E**. The NM-MRI volume is aligned to the brain midline in the coronal and axial images and the AC-PC line in the sagittal image (step 2.8). Part of this figure has been reprinted with permission from Elsevier from [30]. Abbreviations: NM-MRI = neuromelanin-sensitive magnetic resonance imaging; AC-PC = anterior commissure-posterior commissure.

Figure 2: Example of an NM-MRI acquisition that failed the first quality control check (step 3.1 of the protocol). Each of the 20 NM-MRI slices displayed from most inferior (top left image) to most superior (bottom right image); the image window/level was set to exaggerate the contrast between the substantia nigra and crus cerebri. The orange arrows in slices 15–19 show the location of the substantia nigra in those slices. The red arrow in the most superior slice (slice 20) shows that the substantia nigra is still visible in this slice, and thus, the acquisition fails the quality check. Abbreviation: NM-MRI = neuromelanin-sensitive magnetic resonance imaging.

Figure 3: Examples of NM-MRI acquisitions that failed the second quality control check (step 3.2 of the protocol). Only one representative slice is shown for each case. (**A**) An NM-MRI acquisition that fails the quality control check due to a blood vessel artifact (red arrows) that is the result of the blood vessel identified by the blue arrows. (**B**) An NM-MRI acquisition that fails the quality control check due to motion artifacts (red arrows). (**C**) An NM-MRI acquisition that fails the quality control check due to an ambiguous artifact (red arrows). Abbreviation: NM-MRI = neuromelanin-sensitive magnetic resonance imaging.

Figure 4: Example of a representative NM-MRI acquisition. Each of the 20 NM-MRI slices displayed from most inferior (top left image) to most superior (bottom right image); the image window/level was set to exaggerate the contrast between the substantia nigra and crus cerebri from a 28-year-old female participant with no psychiatric or neurological disorders. The NM-MRI protocol ensures complete coverage of the substantia nigra, partial coverage of the locus coeruleus, and satisfactory NM-MRI images. Excellent contrast between the substantia nigra and neighboring white matter regions with no neuromelanin concentration (i.e., crus cerebrus) can

be seen on slices 9–16. The image at the bottom shows a zoomed-in view of the midbrain from slice 13. Abbreviation: NM-MRI = neuromelanin-sensitive magnetic resonance imaging.

DISCUSSION:

The dopaminergic system plays a crucial role in healthy cognition and neuropsychiatric disorders. The development of noninvasive methods that can be used to repeatedly investigate the dopaminergic system *in vivo* is critical for the development of clinically meaningful biomarkers. The protocol described here supplies step-by-step instructions for acquiring good-quality NM-MRI images of the SN, including placement of the NM-MRI volume and quality control checks to ensure usable data.

Notes on analysis of NM-MRI data

Even though detailed protocols for analysis of NM-MRI data have been discussed elsewhere, for completeness, we provide a brief summary of our previous work and recommendations for preprocessing of NM-MRI images and voxelwise analyses. This approach has been validated previously in conjunction with the acquisition protocol described in this paper. Previous studies discuss the advantages of this method in more detail and provide data supporting its reproducibility[6,12,32]. Note however that the standardized acquisition protocol described herein is applicable to any processing and analysis strategy (including ROI-based analysis in native or MNI space[8,32]) and not just the one described here.

For analysis of NM-MRI images, preprocessing can be performed to correct for motion and to spatially normalize individual subject data to a standard anatomical template. We recommend the following pipeline combining Statistical Parametric Mapping (SPM) and Advanced Normalization Tools (ANTs) to use the following tools in the following steps: (1) **SPM-Realign** to realign and correct separately acquired averages for motion, and **SPM-ImCalc** to average the realigned images; (2) **antsBrainExtraction.sh** for brain extraction of the T1w image; (3) **antsRegistrationSyN.sh** (rigid + affine + deformable syn) for spatial normalization of the brain-extracted T1w image to the MNI152NLin2009cAsym template space; (4) **antsRegistrationSyN.sh** (rigid) to coregister the NM-MRI image to the T1w (in native space) image; (5) **antsApplyTransforms** by combining the transformations estimated in steps 3 and 4 into a single-step transformation for spatial normalization of the NM-MRI images to MNI space; and (6) **SPM-Smooth** with a 1 mm full-width-at-half-maximum Gaussian kernel for spatial smoothing of the spatially normalized NM-MRI image. This processing pipeline was previously shown to achieve the highest test-retest reliability in the literature, with an average intra-class correlation coefficient (ICC) within the SN of ~0.90[32]. Furthermore, several previous studies have used similar preprocessing pipelines[12,31,34-37].

After spatial normalization, the NM-MRI images should be analyzed by calculating the contrast-to-noise ratio at each voxel (CNR_V). The CNR measures the percent signal difference between each voxel (I_V) and a reference white matter region known to have little NM content[12] (crus cerebri, I_{CC}), given by the following formula: $CNR_V = \{[I_V - \text{mode}(I_{CC})] / \text{mode}(I_{CC})\}*100$. CNR_V values can be averaged for each participant to determine the CNR of the entire SN or can be analyzed at the voxelwise level within the SN. Higher CNR values reflect increased NM content in

that voxel or ROI. Unlike some other analysis methods that define the SN ROI as the hyperintense region in a NM-MRI image, this recommended method uses predefined template ROIs that can be obtained from the literature[12] or drawn on the average of NM-MRI images in MNI space across all subjects in the study (using a study-specific template). Not only is this method fully automated, it also removes circularity in the analysis, accounts for heterogeneity within the SN-VTA complex, and does not limit analysis to the whole-ROI level.

When acquiring NM-MRI images, it is critical that the T1w images used to place the NM-MRI volume are aligned along the AC-PC line. Doing so will improve the reproducibility of the scans. It is also important to acquire the T1w images as close in time before acquiring the NM-MRI images as possible. Because the T1w image is used for NM-MRI volume placement, it is important that it accurately represents the location of the participant's head in the scanner. If the participant has moved between the T1w scan and the NM-MRI scan, then the NM-MRI volume will not be appropriately placed. Minimizing the amount of time between acquisition of the T1w images and the NM-MRI images will decrease the likelihood that the participant has moved between scans and therefore decrease the likelihood that part of the SN is not included in the NM-MRI volume.

Some modifications to the protocol may be required if issues with the NM-MRI acquisition arise. If the whole SN is not consistently covered, even after correcting the volume placement, then the number of slices in the NM-MRI protocol may need to be increased to capture the entire SN. Additionally, if the participant has difficulty staying still for the entirety of the NM-MRI scan, resulting in consistent motion artifacts, individual repetitions could be acquired and averaged offline. For example, instead of completing one 10-min scan that acquires five repetitions averaged online, five 2-min scans could be acquired and averaged offline. This would give the participant opportunities for breaks in between repetitions and may help them remain still for the duration of the individual scans.

One limitation of this protocol is that it does not provide full coverage of the LC with standard NM-MRI acquisition protocols, preventing the noradrenergic system from being thoroughly investigated using this method. While the LC is a structure that can be imaged using NM-MRI, including the LC in this protocol would increase the number of slices required to reliably capture both the SN and LC in their entirety. Increasing the number of slices would, in turn, increase the scan time for this protocol. Because these scans are sensitive to motion, an increase in scan time may produce lower-quality images as participants may find it more difficult to remain still for longer periods—particularly problematic in clinical populations. Thus, we chose not to include the LC in this protocol to minimize the potential for motion artifacts in the data. Future studies should investigate the reliability of NM-MRI protocols with a greater number of slices to simultaneously image the SN and LC.

A second limitation of this protocol is that the AC-PC alignment of the NM-MRI volume may not provide the optimal orientation for imaging the SN. While the AC-PC line is easy to identify, this orientation does not fully minimize partial volume effects as it is not perfectly perpendicular to the SN. Previous work has utilized an oblique axial section perpendicular to the floor of the fourth

ventricle to image the SN[38-40]. While this volume placement, or one perpendicular to the cerebral aqueduct, may provide less partial volume effects than AC-PC alignment, we chose to use the AC-PC line given its clearly defined landmarks. The validity of this alignment was shown in previous work utilizing the protocol outlined above, in which excellent test-retest reliability was achieved[32]. AC-PC alignment has also been used in several other studies. Cassidy et al. found that patients with cocaine addiction had higher SN CNR values than controls[35]. In a study of patients with late-life depression, Wengler et al. found that psychomotor function was correlated with SN CNR values[36]. A third paper also found that Parkinson's patients had reduced CNR in the SN while patients with psychosis had increased CNR in the SN[12].

However, no study has directly compared different volume placement methods, and this is an area that future research should explore to determine which method provides the best test-retest reliability across multiple acquisitions. 3D NM-MRI sequences could provide an alternative solution because they provide greater flexibility in reformatting after acquisition. Furthermore, 3D sequences achieve a higher signal-to-noise ratio than 2D sequences, potentially allowing for higher spatial resolution but come at the cost of increased sensitivity to motion. Currently, 2D-GRE MT is the only extensively validated NM-MRI sequence—the motivating factor for using it for this protocol. Future studies should compare NM-MRI signal from 3D sequences to NM concentration and striatal dopamine function, and reproducibility in comparison to 2D-GRE MT before widespread adoption.

This protocol has advantages over other NM-MRI protocols because it provides easily identifiable landmarks for NM-MRI volume placement, making it highly reproducible. It also provides online quality checks, which no other NM-MRI protocol has included. These quality checks allow the experimenter to reacquire images if they are of poor quality rather than simply excluding that subject from the analysis.

NM-MRI is a valuable tool that has been used to investigate several neuropsychiatric disorders. NM-MRI is a proxy measure of dopamine function in the nigrostriatal pathway[12], thus offering a method of examining the *in vivo* dopaminergic system that does not require invasive procedures such as PET. Patients with schizophrenia have increased NM signal in the SN[38,41], supporting previous studies that have revealed increased dopaminergic function in schizophrenia. NM-MRI signal in the SN also correlates with psychosis severity in patients with schizophrenia and those at high risk for schizophrenia[12]. Research has also shown that individuals with cocaine use disorder have increased NM-MRI signal in the ventrolateral regions of the SN[35], and that in patients with late-life depression, lower NM-MRI signal in the SN is correlated with motor slowing[36]. Additionally, NM-MRI has been used to study dopaminergic cell loss in conditions such as Parkinson's disease.

Kitao and colleagues established that NM-MRI signal in the SN is correlated with the number of pigmented dopaminergic neurons in the SN[11], and others have shown that NM-MRI signal in SN dopaminergic neurons is decreased in Parkinson's disease[6,9,39,40]. Further research in Parkinson's patients has used NM-MRI to map the topographical pattern of SN cell loss[12] and the progression of SN cell loss over the course of the disease[37]. Altogether, this suggests that not only does NM-

MRI provide insight into the underlying chemical components of neuropsychiatric disorders, but it may also be useful as a biomarker in predicting disease onset and severity. We hope that the standardized protocol presented here will facilitate future work to develop clinically useful biomarkers based on NM-MRI[30].

REFERENCES:

1 Zecca, L. et al. New melanic pigments in the human brain that accumulate in aging and block environmental toxic metals. *Proceedings of the National Academy of Sciences of the United States of America.* **105** (45), 17567–17572 (2008).

2 Zucca, F. A. et al. The neuromelanin of human substantia nigra: physiological and pathogenic aspects. *Pigment Cell Research.* **17** (6), 610–617 (2004).

3 Sulzer, D. et al. Neuromelanin biosynthesis is driven by excess cytosolic catecholamines not accumulated by synaptic vesicles. *Proceedings of the National Academy of Sciences of the United States of America.* **97** (22), 11869–11874 (2000).

4 Cowen, D. The melanoneurons of the human cerebellum (nucleus pigmentosus cerebellaris) and homologues in the monkey. *Journal of Neuropathology & Experimental Neurology.* **45** (3), 205–221 (1986).

5 Zecca, L. et al. The absolute concentration of nigral neuromelanin, assayed by a new sensitive method, increases throughout the life and is dramatically decreased in Parkinson's disease. *FEBS Letters.* **510** (3), 216–220 (2002).

6 Sulzer, D. et al. Neuromelanin detection by magnetic resonance imaging (MRI) and its promise as a biomarker for Parkinson's disease. *NPJ Parkinson's Disease.* **4** (1), 11 (2018).

7 Zucca, F. A. et al. Neuromelanin organelles are specialized autolysosomes that accumulate undegraded proteins and lipids in aging human brain and are likely involved in Parkinson's disease. *NPJ Parkinson's Disease.* **4** (1), 17 (2018).

8 Chen, X. et al. Simultaneous imaging of locus coeruleus and substantia nigra with a quantitative neuromelanin MRI approach. *Magnetic Resonance Imaging.* **32** (10), 1301–1306 (2014).

9 Sasaki, M. et al. Neuromelanin magnetic resonance imaging of locus ceruleus and substantia nigra in Parkinson's disease. *Neuroreport.* **17** (11), 1215–1218 (2006).

10 Trujillo, P. et al. Contrast mechanisms associated with neuromelanin-MRI. *Magnetic Resonance in Medicine.* **78** (5), 1790–1800 (2017).

11 Kitao, S. et al. Correlation between pathology and neuromelanin MR imaging in Parkinson's disease and dementia with Lewy bodies. *Neuroradiology.* **55** (8), 947–953 (2013).

12 Cassidy, C. M. et al. Neuromelanin-sensitive MRI as a noninvasive proxy measure of dopamine function in the human brain. *Proceedings of the National Academy of Sciences of the United States of America.* **116** (11), 5108–5117 (2019).

13 Abi-Dargham, A. et al. Increased striatal dopamine transmission in schizophrenia: confirmation in a second cohort. *American Journal of Psychiatry.* **155** (6), 761–767 (1998).

14 Laruelle, M. et al. Single photon emission computerized tomography imaging of amphetamine-induced dopamine release in drug-free schizophrenic subjects. *Proceedings of the National Academy of Sciences of the United States of America.* **93** (17), 9235–9240 (1996).

15 Breier, A. et al. Schizophrenia is associated with elevated amphetamine-induced synaptic dopamine concentrations: evidence from a novel positron emission tomography method.

Proceedings of the National Academy of Sciences of the United States of America. **94** (6), 2569–2574 (1997).

16 Abi-Dargham, A. et al. Increased baseline occupancy of D-2 receptors by dopamine in schizophrenia. *Proceedings of the National Academy of Sciences of the United States of America.* **97** (14), 8104–8109 (2000).

17 Hietala, J. et al. Presynaptic dopamine function in striatum of neuroleptic-naive schizophrenic patients. *Lancet.* **346** (8983), 1130–1131 (1995).

18 Lindström, L. H. et al. Increased dopamine synthesis rate in medial prefrontal cortex and striatum in schizophrenia indicated by L-(β-11C) DOPA and PET. *Biological Psychiatry.* **46** (5), 681–688 (1999).

19 Meyer-Lindenberg, A. et al. Reduced prefrontal activity predicts exaggerated striatal dopaminergic function in schizophrenia. *Nature Neuroscience.* **5** (3), 267–271 (2002).

20 McGowan, S., Lawrence, A. D., Sales, T., Quested, D., Grasby, P. Presynaptic dopaminergic dysfunction in schizophrenia: a positron emission tomographic [18F] fluorodopa study. *Archives of General Psychiatry.* **61** (2), 134–142 (2004).

21 Bose, S. K. et al. Classification of schizophrenic patients and healthy controls using [18F] fluorodopa PET imaging. *Schizophrenia Research.* **106** (2–3), 148–155 (2008).

22 Kegeles, L. S. et al. Increased synaptic dopamine function in associative regions of the striatum in schizophrenia. *Archives of General Psychiatry.* **67** (3), 231–239 (2010).

23 Toru, M. et al. Neurotransmitters, receptors and neuropeptides in post-mortem brains of chronic schizophrenic patients. *Acta Psychiatrica Scandinavica.* **78** (2), 121–137 (1988).

24 Perez-Costas, E., Melendez-Ferro, M., Rice, M. W., Conley, R. R., Roberts, R. C. Dopamine pathology in schizophrenia: analysis of total and phosphorylated tyrosine hydroxylase in the substantia nigra. *Frontiers in Psychiatry.* **3**, 31 (2012).

25 Howes, O. D. et al. Midbrain dopamine function in schizophrenia and depression: a post-mortem and positron emission tomographic imaging study. *Brain.* **136** (11), 3242–3251 (2013).

26 Bernheimer, H., Birkmayer, W., Hornykiewicz, O., Jellinger, K., Seitelberger, F. Brain dopamine and the syndromes of Parkinson and Huntington Clinical, morphological and neurochemical correlations. *Journal of the Neurological Sciences.* **20** (4), 415–455 (1973).

27 Hirsch, E., Graybiel, A. M., Agid, Y. A. Melanized dopaminergic neurons are differentially susceptible to degeneration in Parkinson's disease. *Nature.* **334** (6180), 345 (1988).

28 Fearnley, J. M., Lees, A. J. Ageing and Parkinson's disease: substantia nigra regional selectivity. *Brain.* **114** (5), 2283–2301 (1991).

29 Damier, P., Hirsch, E., Agid, Y., Graybiel, A. The substantia nigra of the human brain: II. Patterns of loss of dopamine-containing neurons in Parkinson's disease. *Brain.* **122** (8), 1437–1448 (1999).

30 Horga, G., Wengler, K., Cassidy, C. M. Neuromelanin-sensitive magnetic resonance imaging as a proxy marker for catecholamine function in psychiatry. *JAMA Psychiatry.* **78** (7), 788–789 (2021).

31 Wengler, K. et al. Cross-scanner harmonization of neuromelanin-sensitive MRI for multisite studies. *Journal of Magnetic Resonance Imaging.* doi:https://doi.org/10.1002/jmri.27679 (2021).

32 Wengler, K., He, X., Abi-Dargham, A., Horga, G. Reproducibility assessment of neuromelanin-sensitive magnetic resonance imaging protocols for region-of-interest and voxelwise analyses. *NeuroImage.* **208**, 116457 (2020).
33 Griswold, M. A. et al. Generalized autocalibrating partially parallel acquisitions (GRAPPA). *Magnetic Resonance in Medicine.* **47** (6), 1202–1210 (2002).
34 van der Pluijm, M. et al. Reliability and reproducibility of neuromelanin-sensitive imaging of the substantia nigra: a comparison of three different sequences. *Journal of Magnetic Resonance Imaging.* **53** (5), 712–721 (2020).
35 Cassidy, C. M. et al. Evidence for dopamine abnormalities in the substantia nigra in cocaine addiction revealed by neuromelanin-sensitive MRI. *American Journal of Psychiatry.* **177** (11), 1038–1047 (2020).
36 Wengler, K. et al. Association between neuromelanin-sensitive MRI signal and psychomotor slowing in late-life depression. *Neuropsychopharmacology.* **46**, 1233–1239 (2020).
37 Biondetti, E. et al. Spatiotemporal changes in substantia nigra neuromelanin content in Parkinson's disease. *Brain.* **143** (9), 2757–2770 (2020).
38 Shibata, E. et al. Use of neuromelanin-sensitive MRI to distinguish schizophrenic and depressive patients and healthy individuals based on signal alterations in the substantia nigra and locus ceruleus. *Biological Psychiatry.* **64** (5), 401–406 (2008).
39 Fabbri, M. et al. Substantia nigra neuromelanin as an imaging biomarker of disease progression in Parkinson's disease. *Journal of Parkinson's Disease.* **7** (3), 491–501 (2017).
40 Matsuura, K. et al. Neuromelanin magnetic resonance imaging in Parkinson's disease and multiple system atrophy. *European Neurology.* **70** (1–2), 70–77 (2013).
41 Watanabe, Y. et al. Neuromelanin magnetic resonance imaging reveals increased dopaminergic neuron activity in the substantia nigra of patients with schizophrenia. *PLoS One.* **9** (8), e104619 (2014).

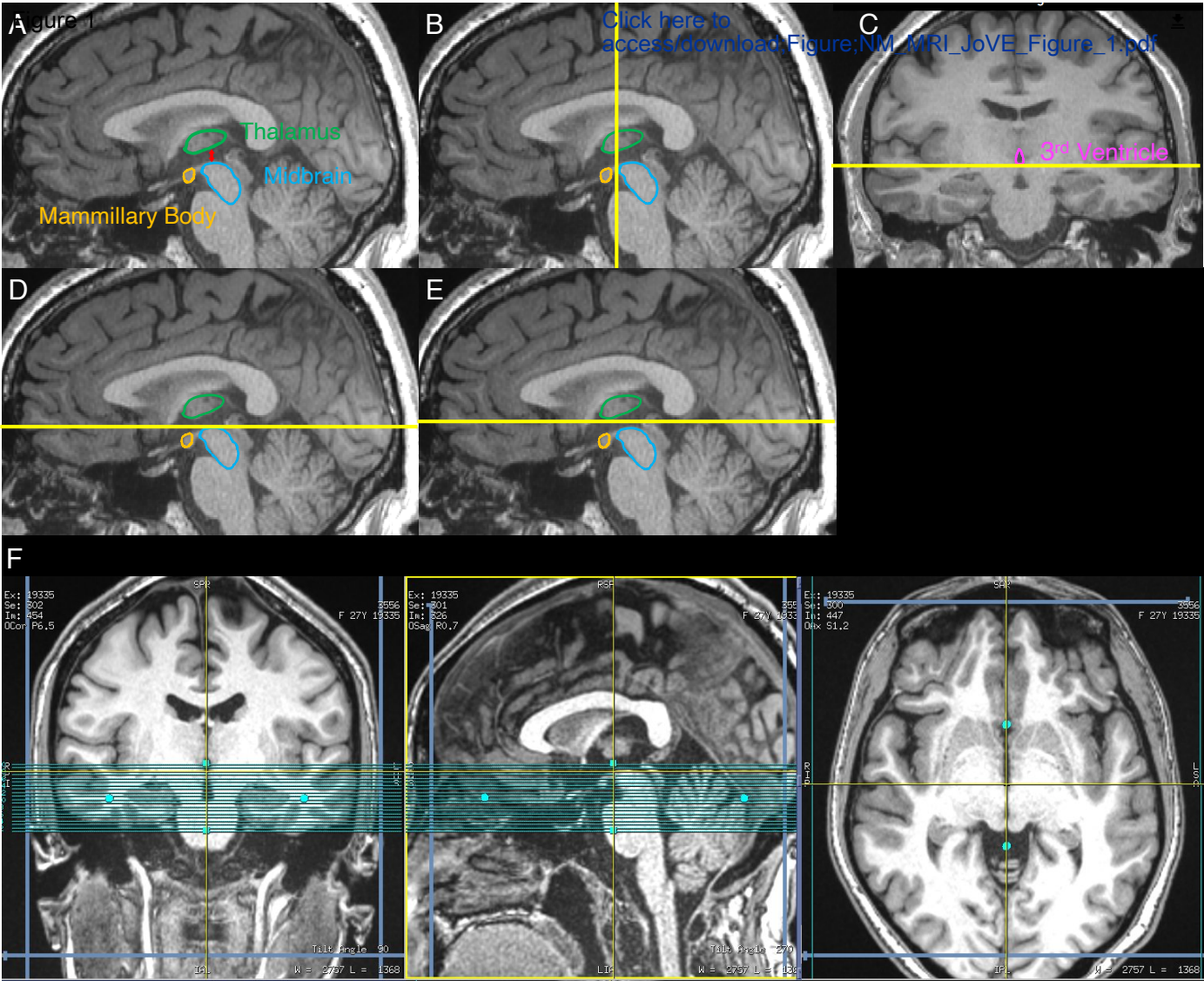
Figure 1
Click here to access/download;Figure;NM_MRI_JoVE_Figure_1.pdf
A
Thalamus
Midbrain
Mammillary Body
B
C
3rd Ventricle
D
E
F

Click here to access/download;Figure;NM_MRI_JoVE_Figure_2.pdf

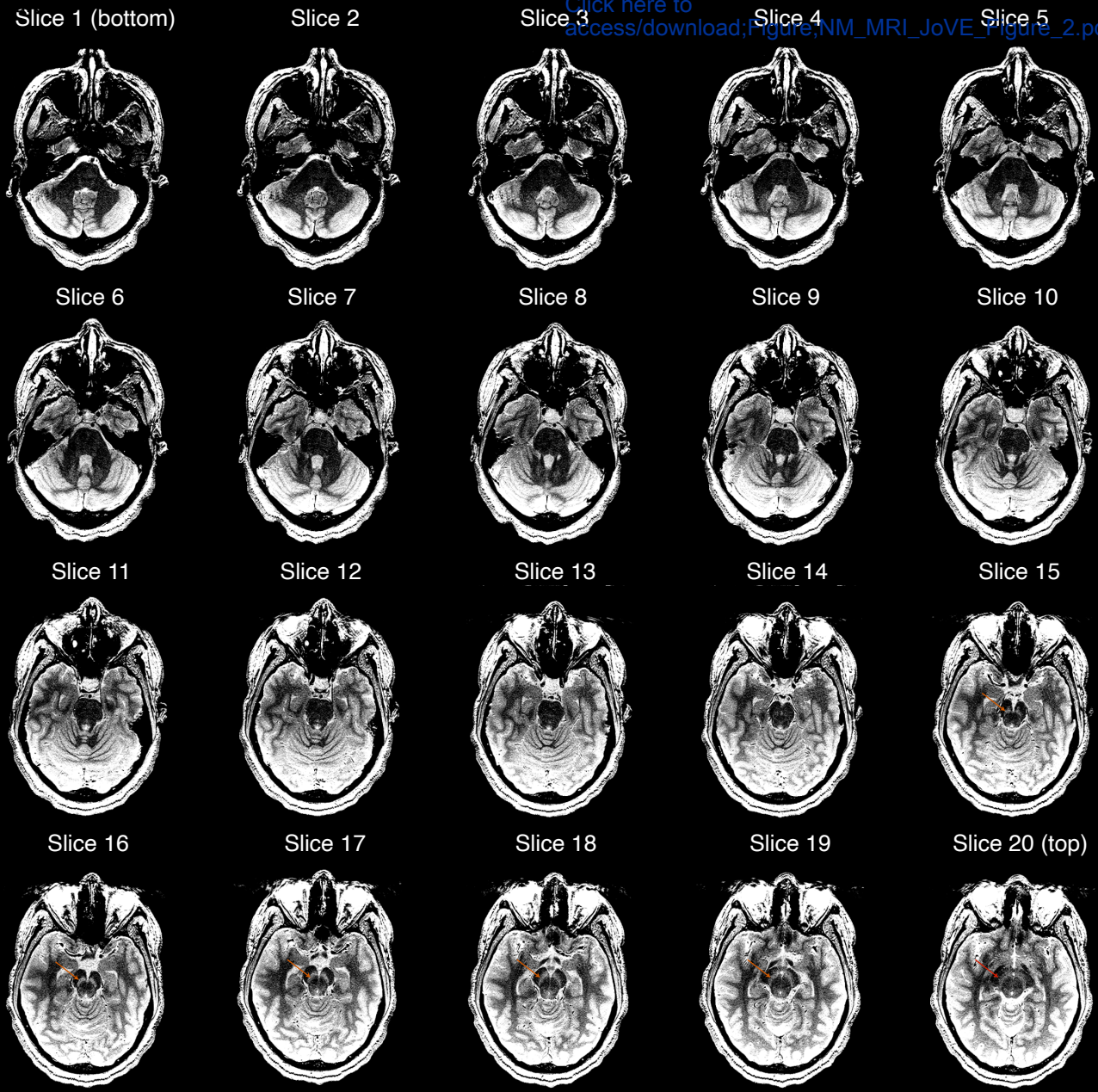

Figure 3

Click here to access/download;Figure;

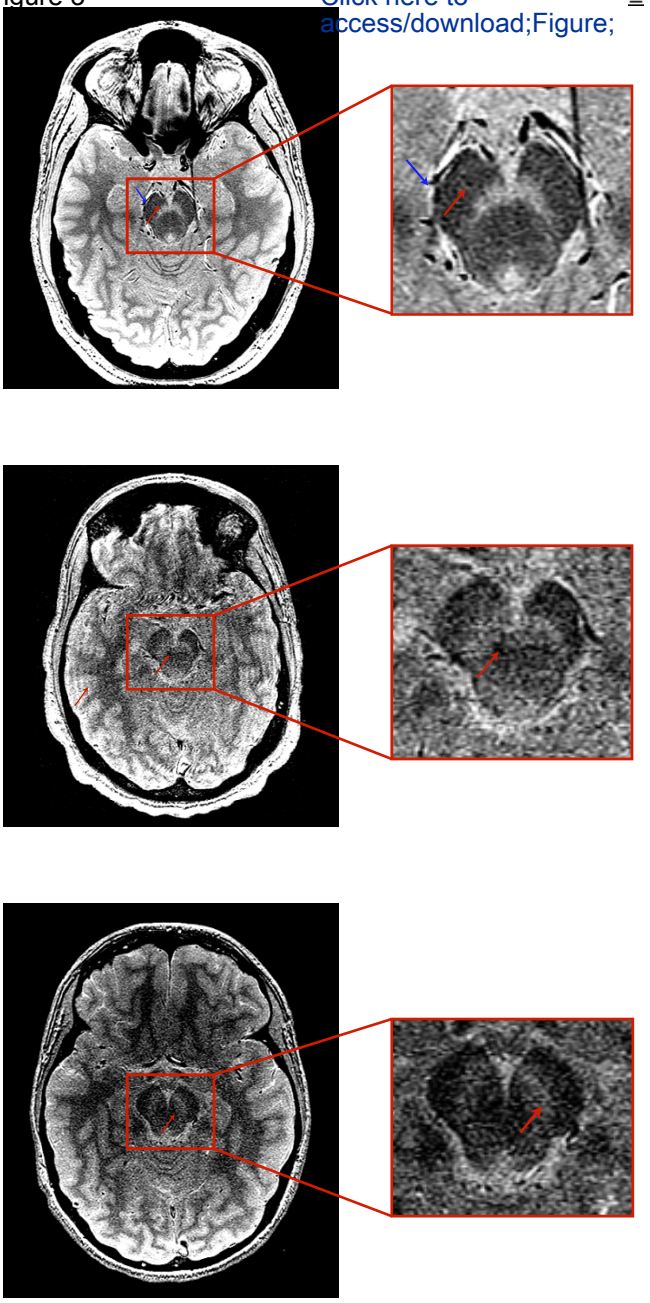

Click here to access/download;Figure;NM_MRI_JoVE_Figure_4.pdf

Slice 1 (bottom) Slice 2 Slice 3 Slice 4 Slice 5

Slice 6 Slice 7 Slice 8 Slice 9 Slice 10

Slice 11 Slice 12 Slice 13 Slice 14 Slice 15

Slice 16 Slice 17 Slice 18 Slice 19 Slice 20 (top)

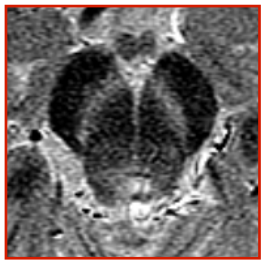

Table of Materials

Click here to access/download
Table of Materials
NM_MRI_JoVE_Table_of_Materials.xls

Rebuttal Letter
Click here to access/download;Rebuttal Letter;JoVE_Response_to_Reviewers2_Final.docx

Dear Editor,

We appreciate the constructive feedback from the reviewers and the opportunity to submit a revised manuscript. We have incorporated or addressed all of the recommended changes into a revised version of the manuscript, which we feel is substantially improved. Changes in the manuscript are indicated as *xxx*. Below we provide point-by-point detailed replies to the reviewers' comments. We hope this revised manuscript is now suitable for publication.

Thank you for your time and consideration.

Sincerely,
Kenneth Wengler, PhD, and Guillermo Horga, MD, PhD

General Response:

We thank the reviewers for their time reviewing our manuscript and their helpful and critical feedback. We have noticed that many of the reviewers' comments, both in this round and the previous round of revisions, has focused on the processing and analysis methods for NM-MRI. The goal of this manuscript was to present a standardized method of acquiring NM-MRI with thorough quality control checks to ensure useable data (rather than to discuss analyses methods in detail that are published elsewhere). NM-MRI has been steadily gaining popularity in the research community and is even gaining significant traction for clinical applications, e.g. in Parkinson's disease. In order to translate NM-MRI into the clinic and for expanded multi-site studies, it is imperative that a standardized acquisition method is used across sites, and the literature to-date has not addressed this issue. We apologize if our overall goal was not fully clear and have made changes to make this more obvious.

A key issue we have with further expanding the manuscript with respect to the processing and analysis methods is that it falls outside the goals of this manuscript and, most importantly, the NM-MRI acquisition protocol that we present can be used for any processing and analysis method, not just the one that we recommend (which was only included at the behest of a reviewer in the previous round of revisions). As such, we would like to avoid adding further details of the processing and analysis approach into this manuscript—all of which have been extensively validated and tested in our previous work (Cassify et al., PNAS 2019; Wengler et al., NeuroImage 2020). We have instead changed the title of the manuscript to "Standardized Data Acquisition for Neuromelanin-sensitive Magnetic Resonance Imaging of the Substantia Nigra," to better reflect the goal of the paper.

Reviewer #2:

Manuscript Summary:

I have no further comments.

Reviewer #3:

Manuscript Summary:

Recent years have wittedness an increased number of NM-MRI papers. This technique has also been used in clinical environments to help the diagnosis of Parkinson's disease. However, we don't often see how the NM volume is placed or how the image quality is checked in published work. Therefore, I appreciate the authors' effort that may lead to better NM-MRI practice. I only have minor comments on the NM-MRI acquisition, but I would like to read more about the preprocessing and ROI analysis.

Major Concerns:

1. Page 9, paragraph 2: Regarding the preprocessing of NM images, could the authors show the quality of coregistration and normalization as figures? Previous studies often measured NM signals on the individual space. It's unclear whether SPM preprocessing works with NM images. It's worth sharing the knowledge.

Response: We appreciate the reviewer pointing this out. Much of our work has indeed been dedicated to the development of the preprocessing pipeline. The pipeline for preprocessing NM-MRI images was extensively tested in our previous work (Wengler et al., NeuroImage, 2020) and was shown to shown to provide excellent test-retest reliability. It is also worth mentioning that multiple recent studies have also used similar voxelwise approaches in MNI space using similar preprocessing pipelines (Cassidy et al., PNAS, 2019; Biondetti et al., Brain, 2020; Sung et al., Human Brain Mapping, 2021; Cassidy et al., AJP, 2021; van der Pluijm et al., JMRI, 2021; Wengler et al., NPP, 2021; Wengler et al., JMRI 2021). The corresponding citations are given in the revised manuscript on page 7.

Furthermore, several previous studies have used similar preprocessing pipelines[12,31,34-37].

Minor Concerns:

2. Page 4, paragraph 1: The authors claim that NM accumulates linearly with age. This claim is inconsistent with recent research on the age effect on NM signals (e.g., Xing et al. 2018, Movement Disorders). I suggest leaving 'linearly' out.

Response: We thank the reviewer for catching this as there does appear to be a nonlinear accumulation, especially in older age (potentially due to neurodegeneration). We have modified this sentence in the revised manuscript accordingly.

It first appears in humans around 2–3 years of age and accumulates with age[1,4,5].

3. Page 4, paragraph 3: The first sentence, "in the SN, NM-MRI can investigate two aspects…", is somewhat misleading. Nm-MRI measures the structural integrity of the SN, but it can not provide a direct measurement of function (e.g., the role of dopamine in reinforcement learning) and cell loss (e.g., counting the number of neurons).

Response: We thank the reviewer for pointing this out as the sentence was a bit misleading. We have revised this statement to more clearly reflect the results in the literature which has shown the NM-MRI contrast in the SN to (1) correlate with the density of neuromelanin-containing neurons in the SN (Kitao et al., Neuroradiology, 2013) and (2) correlate with dopamine-release capacity in the associative striatum (Cassidy et al., PNAS, 2019).

In the SN, NM-MRI can provide a marker of dopaminergic cell loss[11] and indirectly dopamine system function[12].

4. Page 5, paragraph 2: The authors claim that the protocol has been used in several studies. It would be helpful to cite these studies.

Response: We apologize for this oversight. This statement was revised to include the citations and changed to 'multiple' instead of 'several' since some studies have not yet been published.

The protocol outlined in this paper has been utilized in multiple studies[30,31] and was extensively tested.

5. Page 5, paragraph 3: Was it a GE 3T scanner? How long does it take to complete the NM scan with current parameters?

Response: We apologize for forgetting to include this information. Yes, it was a 3T GE scanner and the total acquisition time for the NM-MRI scan was 10 min 4 s. The total acquisition time has been added for both the T1w and NM-MRI sequences. Additional details regarding the MRI scanner are now in the Table of Materials.

T1w: *total acquisition time = 6 min 39 s.*
NM-MRI: *total acquisition time = 10 min 4 s.*

6. Page 6, 1.1: The images were acquired on a GE scanner, but the reformatting has to be done with Siemens or Philips packages? I don't think many institutions have multiple scanners of different producers. Is there a solution with GE or open-source packages?

Response: We apologize for the confusion. This protocol is not specific to any one MRI vendor. Acquisition and reformatting are both done on the same console, examples for

the on-console software were given for both Siemens and Philips, this info has been added for GE.

2.1.1. Carry out online reformatting using the vendor-provided software (e.g., if acquiring data on a GE scanner: MultiPlanar Reconstruction in Planning; if acquiring data on a Siemens scanner: MPR in the 3D Task Card; if acquiring data on a Philips scanner: MPR in the Render Mode of the VolumeView Package).

7. Page 7, 2.1: In Figure 2, the SN is better identified on slices 16-19. Maybe the authors should place red arrows on these slices?

Response: We agree with the reviewer that the SN is better identified on slices 16–19, but the purpose of Figure 2 is to demonstrate the failure of the quality control check detailed in step 3.1 of the protocol ("Ensure that the acquired NM-MRI images cover the entire SN and that the SN is visible in the central images but not in the most superior or most inferior images of the NM-MRI volume."), not to identify out the SN. The red arrow is to denote that the SN is present in the top slice (slice 20); orange arrows have been added to slices 15–19 to denote its location in the other slices.

8. Page 9, paragraph 3: Could the authors recommend an SN template? Speaking from my own experience, SPM extensions such as PickAtlas does not provide a good template of SN, and FreeSurfer subcortical atlas has 'brain-stem' as a whole.

Response: The SN template can either be taken from the literature (e.g., Cassidy et al. PNAS, 2019) or can be hand-drawn on the average NM-MRI image in MNI space across all subjects in the study. The manuscript has been updated for clarity.

Unlike some other analysis methods which define the SN ROI as the hyperintense region in a NM-MRI image, our recommended method uses pre-defined template ROIs that can be obtained from the literature[12] or drawn on the average of NM-MRI images in MNI space across all subjects in the study (using a study-specific template).

Reviewer #4:

Manuscript Summary:

This is my first revision of a manuscript that has been previously reviewed by two other anonymous reviewers. Therefore, in addition to the manuscript, I have also read the

author's rebuttal letter, which has resolved some of my initial doubts. In my opinion, the authors have satisfactorily addressed those original concerns. Likewise, the manuscript is well-written, as well as well-suited and of interest for the journal. However, I have some additional comments that the authors may want to address in a re-revised version of the manuscript.

Major Concerns:

1. Firstly, the authors describe NM contrast as related to the paramagnetic properties of NM, both in isolation or when bound to metals. Although such T1 shortening effects may suffice to explain the bases of NM contrast in SE images, the authors used a GRE sequence with a MT pulse. In this case, in the introduction section, I think the authors should expand their explanation on the bases of the NM signal by discussing MT contrast as the result of the interaction between macromolecular-bound water protons and surrounding free water protons, and how this contrast originates from the selective saturation of macromolecular protons by MT pulses.

Response: We thank the reviewer for pointing this out and apologize for not including greater detail regarding the NM-MRI contrast mechanism. This section has been expanded to include a more detailed description of the MT contrast mechanism believed to drive the NM-MRI signal.

MRI scans that can visualize NM are known as NM-sensitive MRI (NM-MRI) and use either direct or indirect magnetization transfer effects to provide contrast between regions with high NM concentration (e.g., the SN) and the surrounding white matter[8,9]. Magnetization transfer contrast is the result of the interaction between macromolecular-bound water protons (which are saturated by the magnetization transfer pulses) and the surrounding free water protons. In NM-MRI, it is believed that the paramagnetic nature of NM-iron complexes shortens the T1 of the surrounding free water protons resulting in reduced magnetization-transfer effects so that regions with higher NM concentration appear hyperintense on NM-MRI scans[10]. Conversely, the white matter surrounding the SN has a high macromolecular content resulting in large magnetization-transfer effects so the these regions appear hypointense on NM-MRI scans, thus providing high contrast between the SN and surrounding white matter.

2. In the protocol description, please add total acquisition time for each sequence.

Response: We apologize for forgetting to include this information. The total acquisition time for the T1w sequence was 6 min 39 s and for the NM-MRI scan was 10 min 4 s. The total acquisition time has been added for both the T1w and NM-MRI sequences.

T1w: *total acquisition time = 6 min 39 s.*
NM-MRI: *total acquisition time = 10 min 4 s.*

3. I agree with one of the previous reviewers in that the artifact depicted in Figure 3c is quite difficult to notice. Since in this image there are no other apparent signals of acquisition problems (e.g., movement lines, as in Figure 3b) I doubt if re-scanning is needed in this case, since this will, after all, increase acquisition time and therefore increase the likelihood of movement.

Response: We agree that re-acquiring these data are most likely not needed but it is suggested in the event that it was from acquisition problems (e.g., movement lines, as in Figure 3b). Furthermore, if re-acquiring was not necessary, and the re-acquired image has motion artifacts then it would be excluded anyways so there is no practical risk of increased likelihood of movement unless it was necessary to re-acquire the image in the first place. In this case, the experimenter is replacing bad quality data with (potentially) bad quality data, at the cost of increased scan time, but with the potential benefit of getting usable data.

4. The authors recommend realigning the different volumes if averages have been acquired separately. Realign is a function thought for functional time series, and I think here it will be better to co-register the different averages. It should produce similar results, since both algorithms are based on rigid-body transformations.

Response: We thank the reviewer for pointing this out and they are correct that both are rigid-body transformations. While the reviewer is correct that 'Realign' is typically used for functional time series, the appropriate application of this algorithm is for images with the same contrast (like we have here since all are NM-MRI images). Also, the NM-MRI data acquired here can also be thought of as time series, just with much longer separation (typically ~2 min for NM-MRI but ~2 s for fMRI).

5. Also regarding preprocessing, I think steps 3 and 4 should by swapped. I think the logic order is first to co-register T1 and NM images in native space, then normalizing the T1 sequence, and, finally, use this normalization parameters for the co-registered NM sequence.

Response: The current order reflects the steps that the reviewer suggests. The NM-MRI are co-registered to the T1 in T1 native space (not MNI space). This section has been updated for clarity.

(4) coregistration of the NM-MRI image to the T1w (in native space) image using 'antsRegistrationSyN.sh' (rigid);

6. What is the rationale for using a 1mm FWHM smoothing kernel?

Response: Based on previous work (Wengler et al. NeuroImage, 2020), we systematically compared different smoothing kernels and found 1 mm FWHM smoothing kernel to provide the best tradeoff between CNR and ICC.

7. What SN template do the authors suggest for the analysis part?

Response: The SN template can either be taken from the literature (e.g., Cassidy et al. PNAS, 2019) or can be drawn on the average NM-MRI image in MNI space across all subjects in the study. The manuscript has been updated for clarity.

Unlike some other analysis methods which define the SN ROI as the hyperintense region in a NM-MRI image, our recommended method uses pre-defined template ROIs that can be obtained from the literature[12] or drawn on the average of NM-MRI images in MNI space across all subjects in the study (using a study-specific template).

8. How is the reference white matter region defined? How do the authors ensure to avoid including any SN voxel in this reference region? Should the values of this reference region be always averaged and SN values (average or voxel-wise values) compared with this average value? How do the authors suggest to do this comparison if a voxel-wise analysis is preferred? Should each SN be contrasted with an ipsilateral reference region? Does this reference region span a similar number of slices in the rostral-caudal axis (there might be subtle intensity changes across slices acquired at different rostral-caudal levels)? If the reference region only covers a fraction of the SN cluster, this may result in false positive or false negative results.

Response: The reference white matter region (Crus Cerberus; CC) is defined by hand drawing the region surrounding the SN on an average NM-MRI image in MNI space. To overcome the potential issues described by the reviewer, we do not use the average value within the CC (which would be sensitive to including SN edge-voxels or other non-CC voxels as well as the rostral-caudal gradient in the GRE-MT signal) but instead use the mode of the kernel distribution of the CC values. Our previous work showed this method to be the most robust option.

Click here to access/download;Supplemental File (Figures, Permissions, etc.);NM_MRI_JoVE_RightsLink.pdf

ELSEVIER LICENSE
TERMS AND CONDITIONS

Mar 31, 2021

This Agreement between Dr. Kenneth Wengler ("You") and Elsevier ("Elsevier") consists of your license details and the terms and conditions provided by Elsevier and Copyright Clearance Center.

License Number	5039471128844
License date	Mar 31, 2021
Licensed Content Publisher	Elsevier
Licensed Content Publication	NeuroImage
Licensed Content Title	Reproducibility assessment of neuromelanin-sensitive magnetic resonance imaging protocols for region-of-interest and voxelwise analyses
Licensed Content Author	Kenneth Wengler,Xiang He,Anissa Abi-Dargham,Guillermo Horga
Licensed Content Date	Mar 1, 2020
Licensed Content Volume	208
Licensed Content Issue	n/a

Licensed Content Pages	1
Start Page	116457
End Page	0
Type of Use	reuse in a journal/magazine
Requestor type	academic/educational institute
Portion	figures/tables/illustrations
Number of figures/tables/illustrations	1
Format	electronic
Are you the author of this Elsevier article?	Yes
Will you be translating?	No
Title of new article	Neuromelanin-Sensitive Magnetic Resonance Imaging of the Substantia Nigra
Lead author	Kenneth Wengler
Title of targeted journal	Journal of Visualized Experiments
Publisher	Journal of Visualized Experiments
Expected publication	May 2021

date

Portions	Figure 1
Requestor Location	Dr. Kenneth Wengler 1051 Riverside Dr NEW YORK, NY 10032 United States Attn: Dr. Kenneth Wengler
Publisher Tax ID	98-0397604
Total	0.00 USD

Terms and Conditions

INTRODUCTION

1. The publisher for this copyrighted material is Elsevier. By clicking "accept" in connection with completing this licensing transaction, you agree that the following terms and conditions apply to this transaction (along with the Billing and Payment terms and conditions established by Copyright Clearance Center, Inc. ("CCC"), at the time that you opened your Rightslink account and that are available at any time at http://myaccount.copyright.com).

GENERAL TERMS

2. Elsevier hereby grants you permission to reproduce the aforementioned material subject to the terms and conditions indicated.

3. Acknowledgement: If any part of the material to be used (for example, figures) has appeared in our publication with credit or acknowledgement to another source, permission must also be sought from that source. If such permission is not obtained then that material may not be included in your publication/copies. Suitable acknowledgement to the source must be made, either as a footnote or in a reference list at the end of your publication, as follows:

"Reprinted from Publication title, Vol /edition number, Author(s), Title of article / title of chapter, Pages No., Copyright (Year), with permission from Elsevier [OR APPLICABLE SOCIETY COPYRIGHT OWNER]." Also Lancet special credit - "Reprinted from The

Lancet, Vol. number, Author(s), Title of article, Pages No., Copyright (Year), with permission from Elsevier."

4. Reproduction of this material is confined to the purpose and/or media for which permission is hereby given.

5. Altering/Modifying Material: Not Permitted. However figures and illustrations may be altered/adapted minimally to serve your work. Any other abbreviations, additions, deletions and/or any other alterations shall be made only with prior written authorization of Elsevier Ltd. (Please contact Elsevier's permissions helpdesk here). No modifications can be made to any Lancet figures/tables and they must be reproduced in full.

6. If the permission fee for the requested use of our material is waived in this instance, please be advised that your future requests for Elsevier materials may attract a fee.

7. Reservation of Rights: Publisher reserves all rights not specifically granted in the combination of (i) the license details provided by you and accepted in the course of this licensing transaction, (ii) these terms and conditions and (iii) CCC's Billing and Payment terms and conditions.

8. License Contingent Upon Payment: While you may exercise the rights licensed immediately upon issuance of the license at the end of the licensing process for the transaction, provided that you have disclosed complete and accurate details of your proposed use, no license is finally effective unless and until full payment is received from you (either by publisher or by CCC) as provided in CCC's Billing and Payment terms and conditions. If full payment is not received on a timely basis, then any license preliminarily granted shall be deemed automatically revoked and shall be void as if never granted. Further, in the event that you breach any of these terms and conditions or any of CCC's Billing and Payment terms and conditions, the license is automatically revoked and shall be void as if never granted. Use of materials as described in a revoked license, as well as any use of the materials beyond the scope of an unrevoked license, may constitute copyright infringement and publisher reserves the right to take any and all action to protect its copyright in the materials.

9. Warranties: Publisher makes no representations or warranties with respect to the licensed material.

10. Indemnity: You hereby indemnify and agree to hold harmless publisher and CCC, and their respective officers, directors, employees and agents, from and against any and all claims arising out of your use of the licensed material other than as specifically authorized pursuant to this license.

11. No Transfer of License: This license is personal to you and may not be sublicensed, assigned, or transferred by you to any other person without publisher's written permission.

12. No Amendment Except in Writing: This license may not be amended except in a writing signed by both parties (or, in the case of publisher, by CCC on publisher's behalf).

13. Objection to Contrary Terms: Publisher hereby objects to any terms contained in any purchase order, acknowledgment, check endorsement or other writing prepared by you, which terms are inconsistent with these terms and conditions or CCC's Billing and Payment terms and conditions. These terms and conditions, together with CCC's Billing and Payment terms and conditions (which are incorporated herein), comprise the entire agreement between you and publisher (and CCC) concerning this licensing transaction. In the event of any conflict between your obligations established by these terms and conditions and those established by CCC's Billing and Payment terms and conditions, these terms and conditions shall control.

14. Revocation: Elsevier or Copyright Clearance Center may deny the permissions described in this License at their sole discretion, for any reason or no reason, with a full refund payable to you. Notice of such denial will be made using the contact information provided by you. Failure to receive such notice will not alter or invalidate the denial. In no event will Elsevier or Copyright Clearance Center be responsible or liable for any costs, expenses or damage incurred by you as a result of a denial of your permission request, other than a refund of the amount(s) paid by you to Elsevier and/or Copyright Clearance Center for denied permissions.

LIMITED LICENSE

The following terms and conditions apply only to specific license types:

15. **Translation**: This permission is granted for non-exclusive world **English** rights only unless your license was granted for translation rights. If you licensed translation rights you may only translate this content into the languages you requested. A professional translator must perform all translations and reproduce the content word for word preserving the integrity of the article.

16. **Posting licensed content on any Website**: The following terms and conditions apply as follows: Licensing material from an Elsevier journal: All content posted to the web site must maintain the copyright information line on the bottom of each image; A hyper-text must be included to the Homepage of the journal from which you are licensing at http://www.sciencedirect.com/science/journal/xxxxx or the Elsevier homepage for books at http://www.elsevier.com; Central Storage: This license does not include permission for a scanned version of the material to be stored in a central repository such as that provided by Heron/XanEdu.

Licensing material from an Elsevier book: A hyper-text link must be included to the Elsevier homepage at http://www.elsevier.com . All content posted to the web site must maintain the copyright information line on the bottom of each image.

Posting licensed content on Electronic reserve: In addition to the above the following clauses are applicable: The web site must be password-protected and made available only to bona fide students registered on a relevant course. This permission is granted for 1 year only. You may obtain a new license for future website posting.

17. **For journal authors:** the following clauses are applicable in addition to the above:

Preprints:

A preprint is an author's own write-up of research results and analysis, it has not been peer-reviewed, nor has it had any other value added to it by a publisher (such as formatting, copyright, technical enhancement etc.).

Authors can share their preprints anywhere at any time. Preprints should not be added to or enhanced in any way in order to appear more like, or to substitute for, the final versions of articles however authors can update their preprints on arXiv or RePEc with their Accepted Author Manuscript (see below).

If accepted for publication, we encourage authors to link from the preprint to their formal publication via its DOI. Millions of researchers have access to the formal publications on ScienceDirect, and so links will help users to find, access, cite and use the best available version. Please note that Cell Press, The Lancet and some society-owned have different preprint policies. Information on these policies is available on the journal homepage.

Accepted Author Manuscripts: An accepted author manuscript is the manuscript of an article that has been accepted for publication and which typically includes author-incorporated changes suggested during submission, peer review and editor-author communications.

Authors can share their accepted author manuscript:

- immediately
    - via their non-commercial person homepage or blog
    - by updating a preprint in arXiv or RePEc with the accepted manuscript
    - via their research institute or institutional repository for internal institutional uses or as part of an invitation-only research collaboration work-group
    - directly by providing copies to their students or to research collaborators for their personal use
    - for private scholarly sharing as part of an invitation-only work group on commercial sites with which Elsevier has an agreement
- After the embargo period
    - via non-commercial hosting platforms such as their institutional repository
    - via commercial sites with which Elsevier has an agreement

In all cases accepted manuscripts should:

- link to the formal publication via its DOI
- bear a CC-BY-NC-ND license - this is easy to do
- if aggregated with other manuscripts, for example in a repository or other site, be shared in alignment with our hosting policy not be added to or enhanced in any way to appear more like, or to substitute for, the published journal article.

Published journal article (JPA): A published journal article (PJA) is the definitive final

record of published research that appears or will appear in the journal and embodies all value-adding publishing activities including peer review co-ordination, copy-editing, formatting, (if relevant) pagination and online enrichment.

Policies for sharing publishing journal articles differ for subscription and gold open access articles:

Subscription Articles: If you are an author, please share a link to your article rather than the full-text. Millions of researchers have access to the formal publications on ScienceDirect, and so links will help your users to find, access, cite, and use the best available version.

Theses and dissertations which contain embedded PJAs as part of the formal submission can be posted publicly by the awarding institution with DOI links back to the formal publications on ScienceDirect.

If you are affiliated with a library that subscribes to ScienceDirect you have additional private sharing rights for others' research accessed under that agreement. This includes use for classroom teaching and internal training at the institution (including use in course packs and courseware programs), and inclusion of the article for grant funding purposes.

Gold Open Access Articles: May be shared according to the author-selected end-user license and should contain a CrossMark logo, the end user license, and a DOI link to the formal publication on ScienceDirect.

Please refer to Elsevier's posting policy for further information.

18. **For book authors** the following clauses are applicable in addition to the above: Authors are permitted to place a brief summary of their work online only. You are not allowed to download and post the published electronic version of your chapter, nor may you scan the printed edition to create an electronic version. **Posting to a repository:** Authors are permitted to post a summary of their chapter only in their institution's repository.

19. **Thesis/Dissertation**: If your license is for use in a thesis/dissertation your thesis may be submitted to your institution in either print or electronic form. Should your thesis be published commercially, please reapply for permission. These requirements include permission for the Library and Archives of Canada to supply single copies, on demand, of the complete thesis and include permission for Proquest/UMI to supply single copies, on demand, of the complete thesis. Should your thesis be published commercially, please reapply for permission. Theses and dissertations which contain embedded PJAs as part of the formal submission can be posted publicly by the awarding institution with DOI links back to the formal publications on ScienceDirect.

Elsevier Open Access Terms and Conditions

You can publish open access with Elsevier in hundreds of open access journals or in nearly 2000 established subscription journals that support open access publishing. Permitted third

party re-use of these open access articles is defined by the author's choice of Creative Commons user license. See our open access license policy for more information.

Terms & Conditions applicable to all Open Access articles published with Elsevier:

Any reuse of the article must not represent the author as endorsing the adaptation of the article nor should the article be modified in such a way as to damage the author's honour or reputation. If any changes have been made, such changes must be clearly indicated.

The author(s) must be appropriately credited and we ask that you include the end user license and a DOI link to the formal publication on ScienceDirect.

If any part of the material to be used (for example, figures) has appeared in our publication with credit or acknowledgement to another source it is the responsibility of the user to ensure their reuse complies with the terms and conditions determined by the rights holder.

Additional Terms & Conditions applicable to each Creative Commons user license:

CC BY: The CC-BY license allows users to copy, to create extracts, abstracts and new works from the Article, to alter and revise the Article and to make commercial use of the Article (including reuse and/or resale of the Article by commercial entities), provided the user gives appropriate credit (with a link to the formal publication through the relevant DOI), provides a link to the license, indicates if changes were made and the licensor is not represented as endorsing the use made of the work. The full details of the license are available at http://creativecommons.org/licenses/by/4.0.

CC BY NC SA: The CC BY-NC-SA license allows users to copy, to create extracts, abstracts and new works from the Article, to alter and revise the Article, provided this is not done for commercial purposes, and that the user gives appropriate credit (with a link to the formal publication through the relevant DOI), provides a link to the license, indicates if changes were made and the licensor is not represented as endorsing the use made of the work. Further, any new works must be made available on the same conditions. The full details of the license are available at http://creativecommons.org/licenses/by-nc-sa/4.0.

CC BY NC ND: The CC BY-NC-ND license allows users to copy and distribute the Article, provided this is not done for commercial purposes and further does not permit distribution of the Article if it is changed or edited in any way, and provided the user gives appropriate credit (with a link to the formal publication through the relevant DOI), provides a link to the license, and that the licensor is not represented as endorsing the use made of the work. The full details of the license are available at http://creativecommons.org/licenses/by-nc-nd/4.0. Any commercial reuse of Open Access articles published with a CC BY NC SA or CC BY NC ND license requires permission from Elsevier and will be subject to a fee.

Commercial reuse includes:

- Associating advertising with the full text of the Article
- Charging fees for document delivery or access
- Article aggregation

- Systematic distribution via e-mail lists or share buttons

Posting or linking by commercial companies for use by customers of those companies.

20. **Other Conditions**:

v1.10

Questions? customercare@copyright.com or +1-855-239-3415 (toll free in the US) or +1-978-646-2777.